Laurent Jacquin
(Onera)

E-mail: laurent.jacquin@onera.fr

Scales in Turbulent Motions

This paper reviews some of the classical dimensional principles used in fluid mechanics to predict the characteristic scales of turbulent flows. The reasoning makes largely reference to the celebrated Kolmogorov theory we first briefly recall. Data obtained in two wind tunnel experiments are then used to exemplify the concepts and to provide typical values of the different length and time scales involved in wind tunnel experiments. Measurement techniques and their role in the scientific research in fluid mechanics are then succinctly commented.

Navier-Stokes equations and the Reynolds number

Navier-Stokes equations correspond to the fundamental law of dynamics applied to a fluid particle (in mechanics, 'particle' means a macroscopic set of molecules of undefined shape and size). For a flow of an incompressible fluid with no volume force, the most standard form of the Navier-Stokes equation is:

$$\underline{u}_{,t} + \nabla \underline{u}.\underline{u} = -\frac{1}{\rho}\underline{grad}\ p + \nu \Delta \underline{u} \qquad (1)$$

In this equation $\underline{u}(\underline{x},t)$ denotes the velocity vector of the fluid particle, $\underline{u}_{,t}$ its temporal variation, $\nabla \underline{u}$ its gradient, ρ the fluid density, p, its pressure and ν its kinematic viscosity. The left hand side of equation (1) is the acceleration of the particle. This acceleration comprises two terms: a variation with time and a variation in space. The flow is steady (or permanent) if the first term is zero; however, this does not prevent the velocity from varying locally in space through the second term, called convective acceleration. The right hand side of equation (1) characterizes the only two mechanisms that can influence the motion of the particle in the absence of volume forces, i.e. the non-homogeneity of the pressure and the viscous diffusion of the momentum. Pressure is a scalar and is involved in equation (1) through a gradient (the particle is accelerated towards the low pressure regions of the flow). As for the second term, it logically takes the form of a Laplacian affected by a diffusion coefficient, which is here the kinematic viscosity of the fluid.

The main difficulty in fluid mechanics relies in the non-linear nature of the acceleration term $\nabla \underline{u}.\underline{u}$ of equation (1). We can only avoid this difficulty when this term is negligible with respect to the viscous diffusion (the last term of (1); the pressure term adapts to the velocity and is therefore not a scaling term). If we introduce the characteristic scales $|\underline{u}| \propto U$ and $|\nabla| \propto 1/l$, the ratio between these two terms is evaluated as:

$$\mathrm{Re} = \frac{|\nabla \underline{u}.\underline{u}|}{|\nu \Delta \underline{u}|} \propto \frac{U^2/l}{\nu U/l^2} = \frac{U\,l}{\nu} \qquad (2)$$

This dimensionless parameter defines the Reynolds number. When $\mathrm{Re} << 1$, the flow is dominated by viscosity and the equations become linear. Observations and theory show that the corresponding flows are generally stable to unsteady perturbations. Starting from this situation, when we increase the Reynolds number, flows progressively destabilize and then turbulence appears. Typically, flows are fully turbulent when $\mathrm{Re} >> 1$ (there are exceptions however, the vortex being an example).

Turbulence

The dissipative and irreversible nature of a fluid motion is due to viscosity. This may be understood if we consider the power per unit mass developed by the viscous friction in equation (1). This power, expressed as $P = \underline{u}.(\nu \Delta \underline{u})$. Simple vector manipulations allow to separate it into two terms:

$$P = \underline{u}.(\nu \Delta \underline{u}) = \nu \Delta\left(\tfrac{1}{2}\underline{u}^2\right) - \nu |\nabla \underline{u}|^2 \qquad (3)$$

We see that viscosity has two effects: it diffuses the kinetic energy in space through the first term, while reducing it with the second term:

$$\varepsilon = \nu\ |\nabla \underline{u}|^2 \qquad (4)$$

This term, defined as positive, is involved in the rate of dissipation of kinetic energy per unit mass. It expresses the irreversible nature of the movement (we find it with an opposite sign in the internal energy and entropy equations). Importantly, (4) shows that dissipation of energy requires high velocity gradients $|\nabla \underline{u}|$, and is thus ascribed to small scale activity. Turbulence is a phenomenon that indeed allows for the development of small scales and intense gradients, which are needed to dissipate energy. The concept of turbulence then leads to a paradox which we can summarize now, instructively.

This paradox appears, for example, when we evaluate the energy dissipated by the movement of an object in a fluid, a sphere in the example of Figure 1. This energy corresponds to the work of the drag force that opposes the motion of the object through the fluid.

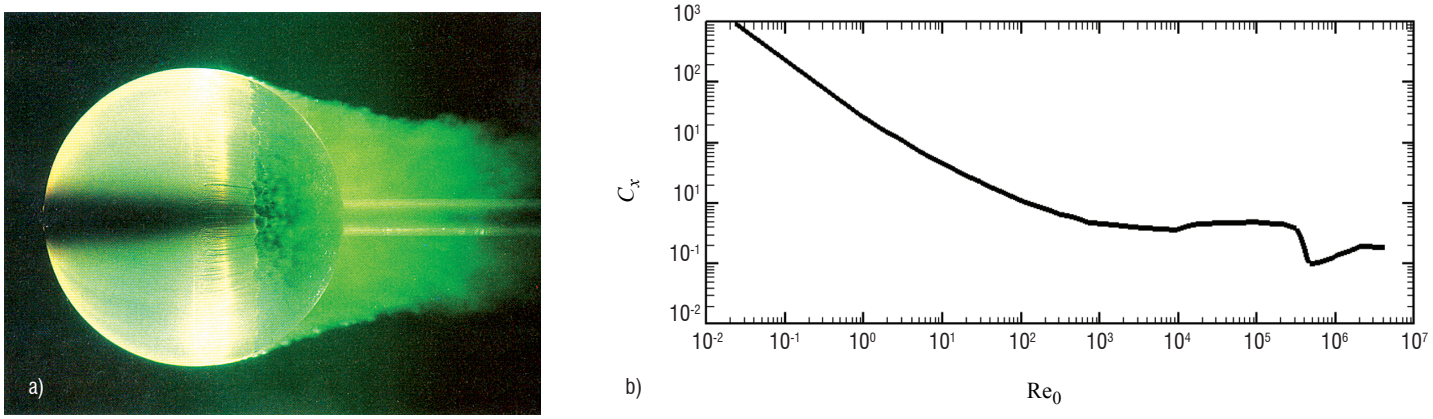

Figure 1 – Influence of the Reynolds number $\mathrm{Re}_0 = U_0 D/\nu$ on the flow around a smooth sphere (U_0 is the speed of flow far upstream of the sphere and D, the diameter of the sphere): (a) dye visualization by colorant in a hydraulic tank for $\mathrm{Re}_0 \approx 400\,000$ (Werlé, 1987), (b) drag coefficient of the sphere $C_x = F_x \Big/ \left(\frac{1}{2}\rho U_0^2 D^2\right)$ as a function of Re_0.

Supposing a sphere of diameter D fixed in a flow of speed U_0 of a fluid of density ρ and kinematic viscosity ν, if we express the three physical dimensions involved in this problem (mass, length and time) using ρ, U_0 and D, the drag force can be written in the form:

$$F_x = C_x(\mathrm{Re}_0)\rho U_0^2 D^2 \qquad (5)$$

The dimensionless coefficient C_x is the drag coefficient. It only depends on the Reynolds number $\mathrm{Re}_0 = U_0 D/\nu$. The power developed by this force, $F_x\ U_0$, is equal to the rate of energy dissipated within the flow. If we consider an average in a volume of fluid $V \sim D^3$ and build the rate of dissipation per unit mass, we obtain:

$$<\varepsilon> = \frac{F_x\ U_0}{\rho V} = C_x(\mathrm{Re})\frac{U_0^3}{D} \qquad (6)$$

To this day, there exists no theory allowing us to go beyond these laws and we must use experiments to determine the behavior of the unknown function $C_x(\mathrm{Re})$. Figure 1b shows the result for the flow past the sphere. The behavior obtained for $\mathrm{Re} \to 0$ is logical: the more viscous the fluid, the more energy must be dissipated to move in it. On the other hand, the saturation of C_x at high Reynolds numbers is not intuitive. We will see that it is in fact quite surprising.

Returning to (6), the experiment of Figure 1b shows that

$\lim_{\mathrm{Re}>>1} C_x(\mathrm{Re}) \approx Cte$, so that:

$$\lim_{\mathrm{Re}>>1} <\varepsilon> \approx Cte \times \frac{U_0^3}{D} \qquad (7)$$

We conclude that at high Reynolds numbers, the power per unit mass absorbed by the viscous friction becomes independent of the viscosity ! This is the very paradox we mentioned. Following (7), this power becomes equal to a constant fraction of the power U_0^3/D injected during the interaction between the object of size D and the flow of velocity U_0; it does not depend on anything else, especially not on the viscosity. Furthermore, in light of (4), relation (7) is equivalent to $\lim_{\nu \to 0} <\nu\ |\nabla \underline{u}|^2> \approx Cte$ which implies that the flow would be capable of developing singularities ($|\nabla \underline{u}| \to \infty$) in the limit case where $\nu \to 0$. Richardson (1922) and Kolmogorov (1941) contributed to assemble these elements into a phenomenological model which unravels the paradox mentioned above. This model, referred to as the Richardson-Kolmogorov cascade, constitutes an essential basis for the interpretation of the physics, and thus the measurement, of turbulent fluid flows.

The model is based on the principle of a fragmentation of scales that adjusts the rate of the energy dissipated within the flow volume to the power developed by externally imposed forces. Sticking to the essential points, in the Richardson-Kolmogorov cascade model turbulence is viewed as a set of imbricated “fluid structures” whose characteristic size decreases according to a dynamic process of successive fragmentations of the structures into smaller and smaller structures. This model is shown schematically in Figure 2. In this way, the

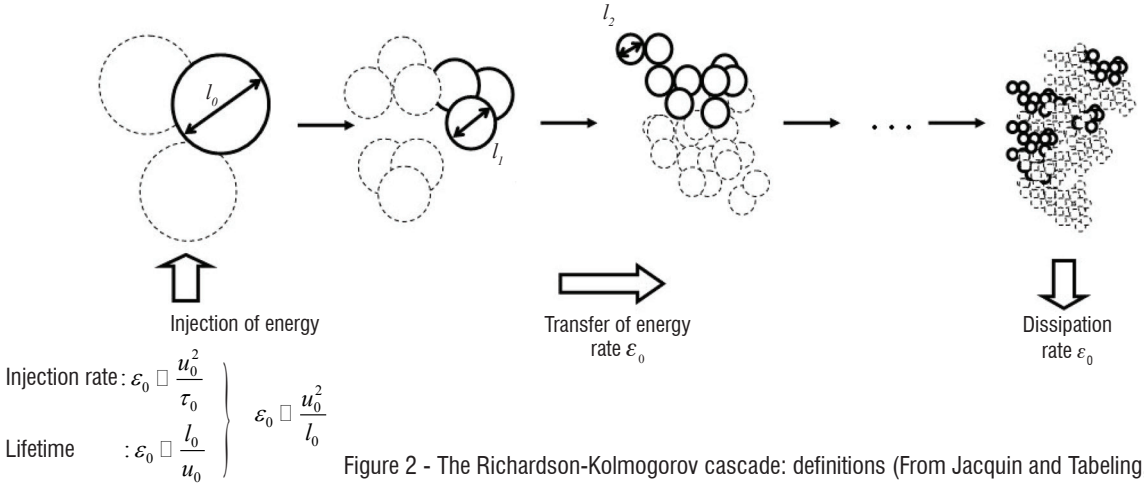

Figure 2 - The Richardson-Kolmogorov cascade: definitions (From Jacquin and Tabeling, 2006)

kinetic energy of the largest scales of characteristic length l_0 and velocity u_0 and on which external forces act, is transferred to the small scales of the motion. In the case of the wake of the sphere of Figure 1, we can consider that these largest scales of the turbulent movement verify: $l_0 \sim D$, $u_0 \sim U_0$. The rate of energy transfer per unit mass is thus in this case:

$$\varepsilon_0 \sim U_0^3 / D \qquad (8)$$

Through this process of scale fragmentation, the kinetic energy per unit mass U_0^2 is transferred from scale to scale without any loss until turbulent structures become small enough to be eliminated by the viscous friction. There, the energy will be finally transformed into heat. Thus, in this cascade, it is not energy that is conserved from scales to scales, but the rate of transfer of this energy. This rate remains constant and equal to ε_0 (see Figure 2). The characteristic velocity scale u_l of the structures of size l is given, whatever l, by the relation $\varepsilon_l \sim u_l^3 / l \sim \varepsilon_0$ or:

$$u_l \sim (\varepsilon_0 l)^{1/3} \qquad (9)$$

For the velocity gradients, we obtain $\nabla u_l \sim u_l / l \sim l^{-2/3}$. According to this law, the decrease in the flow scales within the cascade process is as a matter of fact able to produce the gradients which are necessary to dissipate the energy, see (4).

Figure 3 provides an example that illustrates the relevance of this model in a complex flow. It shows results based on the measurement of the three components of the velocity by PIV in a massive turbulent separation region over a rounded ramp. The geometry of the channel and the mean velocity field determined in several vertical cross sections are shown in Figure 3a. Averaging is made on a set of 1000 images for each of the planes. The images are recorded using a 1376 pixel x 1040 pixel digital camera and the velocity is determined by a standard cross-correlation method. An analysis of the turbulent behavior is done in an exploration window of 100 mm x 200 mm located in the lower part of the section at x = 450 mm. Figure 3b shows the longitudinal velocity averaged on 1000 images. This averaged field corresponds to a shear. Figure 3c isolates one of the images. The variable represented in this latter Figure is not the velocity but the component of the vorticity perpendicular to the observation plane, $\omega_x = \partial V / \partial x - \partial U / \partial y$.

We see that the turbulent vorticity 'superimposed' on the mean shear of Figure 3b presents a very fragmentary and homogeneous aspect that does not in any way reflect the average structure of the flow. Note that in these first three figures, the spatial resolution of PIV is determined by the size N = 32 x 32 pixel² assigned to the interrogation window ; the corresponding physical scale is about $L \approx 3$ mm. In Figure 3d, we show the result of an exploration of the scales of this turbulent motion made by modulating the resolution of PIV between N = 16 pixels ($L \approx 1.5$ mm) and N = 512 pixels ($L \approx 48$ mm). We plot in this Figure $\log < |\omega_x| >$ as a function of $\log N$. In accordance with (9), the theory provides the following scaling law for the vorticity:

$$\omega_l \sim \frac{u_l}{l} \sim l^{-2/3} \qquad (10)$$

We see in Figure 3d that the observations correctly reproduce this behavior. Thus, there is a fluctuating movement superimposed on

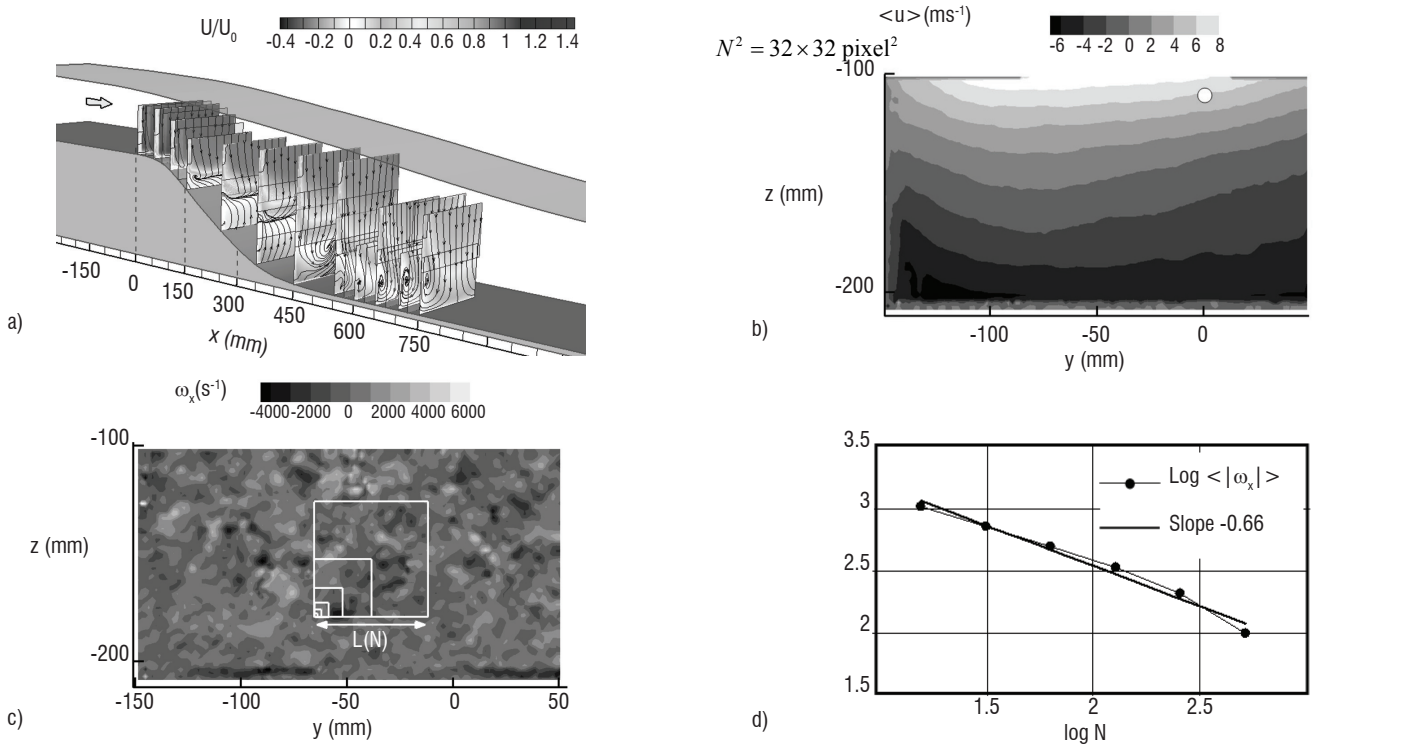

Figure 3 – Separated flow in a curved channel: (a) channel geometry, mean longitudinal velocity and projected stream lines obtained by 3C PIV in planes perpendicular to the upstream flow (averaging is made on 1000 images), (b) mean longitudinal velocity in the plane x = 450 mm (resolution: N^2= 32x32 pixel²), (c) longitudinal component of the fluctuation of instantaneous vorticity measured in the same window as Figure b (resolution: N^2= 32x32 pixel²), (d) average of the absolute value of the vorticity ω_x as a function of N for $N = 2^n$ and n = 4-9, log-log plot. The physical sizes $L(N)$ of these windows are shown in superimposition in Figure 3c. The white circle in Figure 3b indicates the point of coordinates (x = 450 mm, y = 0, z = -127 mm) where the spectrum of Figure 4 is determined. Figure 3a is taken from Gardarin and Jacquin (2008).

the well structured mean shear of Figure 3b, which is fragmented according to the scheme of the Richardson-Kolmogorov cascade. Through (10), this movement may be seen as a vorticity field with an intensity which varies as the power -2/3 of the vortex scale. This means that turbulence can be seen as a distribution of more and more intermittent and singular vortices as we refine the scale of observation. The limit of this fragmentation is fixed by a minimum scale where viscous regularization can take place.

The smallest scales of the flow

The Kolmogorov scale

The limit of the inertial process described above is fixed by viscosity which selects the smallest scales of the motion. These scales, of size $l_{\min}$ and characteristic velocity $u_{\min}$, are those for which the Reynolds number is of order unity, $\mathrm{Re}_{\min} = u_{\min} l_{\min} / \nu \approx 1$: in accordance with (2), in these conditions viscosity once again becomes efficient and transforms the kinetic energy into heat. By combining this relation with $\varepsilon_0 \sim u_{\min}^3 / l_{\min}$, we find that the smallest possible scales verify:

$$l_{\min} \sim \left(\nu^3 / \varepsilon_0\right)^{1/4} \equiv \eta \qquad (11)$$

This is the Kolmogorov scale. By combining (8) and (11), we find that the ratio between the largest scale l_0 and the smallest one, η, is:

$$\frac{l_0}{\eta} \sim \mathrm{Re}_0^{3/4} \qquad (12)$$

This demonstrates that the extent of the range of cascading scales adapts to the Reynolds number by evolving as its power 3/4.

As an example, for the wake of the sphere of Figure 2, where $\mathrm{Re}_0 \approx 400\,000$, if we consider a diameter of $l_0 = 0.1$ m (say, an average scale for a sport ball), we obtain $\eta \approx 6\mu m$. At a fixed point located in the turbulent wake of this sphere, the measured frequencies are obtained by taking the local convection velocity of the scales l_0 and η. By taking for this velocity the upstream velocity $U_0 \approx 5$ ms^{-1}, the frequencies obtained are $f_0 \approx U_0 / l_0 \approx 40$ Hz, for the largest scale, and $f_\eta \approx U_0 / \eta \approx 640$ kHz (!) for the smallest one. These are the characteristic scales of this flow.

In the channel flow of Figure 3, at the point of coordinates (x = 450 mm, y = 0, z = -127 mm) indicated in Figure 3b, if we take as a characteristic velocity the difference in the velocities that shears the flow, here $u_0 \approx 30$ ms^{-1}, and if we consider that the scale of energy injection is $l_0 \approx 0.2$ m (the height of the rounded ramp), we obtain the same Reynolds number as previously, $\mathrm{Re}_0 \approx 400\,000$. (12) then yields $\eta \approx 12\ \mu m$ for the Kolmogorov scale. At this point, the local convection velocity is $U_0 \approx 5$ ms^{-1} (see Figure 3b) so that, in terms of frequency, the limits of the turbulent cascade are equivalent to the preceding ones: $f_0 \approx U_0 / l_0 \approx 25$ Hz and $f_\eta \approx U_0 / \eta \approx 417$ kHz.

Figure 4 shows the power spectral density of the fluctuations of the longitudinal velocity measured with a hot-wire probe placed at the point represented in Figure 3b. The hot-wire technique is based on the measurement of voltage variations at the tips of a small heated metallic filament in which a current is modulated so as to maintain a constant temperature of the filament. The voltage fluctuations are proportional to the variations of the flow velocity, that influences the filament temperature, and thus its resistance. This miniature sensor has a low enough thermal inertia to allow resolution of the small spatial and temporal scales of a turbulent flow (when the mean convection velocity is not too large). The hot-wire probe signal is here acquired with a frequency of 9 kHz. It is low-pass filtered with a cut-off frequency of f_c=2 kHz (here, this low value was sufficient for the author's purposes; note that in this flow a hot wire could discriminate the scales up to a frequency of more than 10 kHz). Beyond the frequency f_0 where energy is injected, the spectral density follows the famous "-5/3" power law predicted by the Richardson-Kolmogorov model (the demonstration may be found in any text book dealing with turbulence; see e.g. Jacquin and Tabeling, 2006, in French). The measurement is here under-resolved because, as shown by the theoretical dotted line, the cascade continues until the viscous frequency f_η which is well beyond the low-pass cut-off of the filter. However, the contribution to the total energy of the unresolved scales located in the range $f_c \le f \le f_\eta$ can be considered as negligible. We also see in gray in this Figure the range of the inertial scales of the cascade accounted for by PIV according to the scale of resolution L ($N = 2^n$) with η = 4-9 as indicated in Figure 3c.

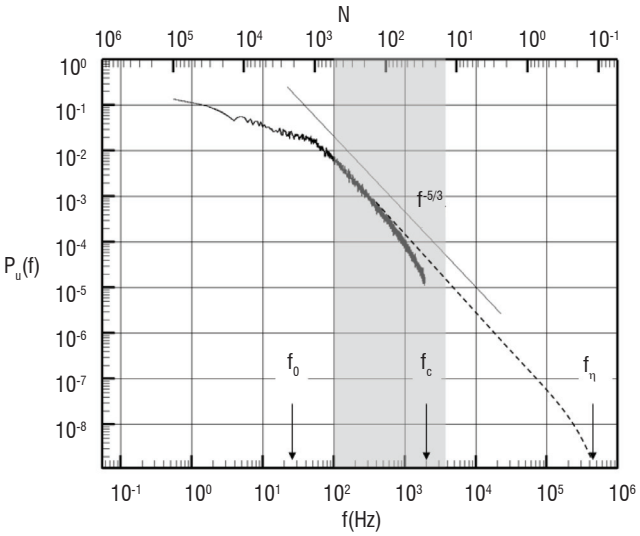

Figure 4 - Power spectral density of the velocity fluctuations at the point indicated in Figure 3b. Solid line: hot-wire measurement (acquisition at frequency f_{acq} = 9 kHz, low-pass filtering at f_{acq} = 2 kHz); dotted line: non-resolved part. The turbulent energy cascade theoretically develops between frequencies $f_0 \approx U_0 / l_0$ 25 Hz and $f_\eta \approx U_0 / \eta \approx 417$ kHz. The gray band represents the frequencies covered by the PIV resolutions tested in Figure 3.

It must be realized that while the cascade produces finer and finer and more intense vortices ($\omega_l \sim l^{-2/3}$, see (10)), these vortices carry less and less energy ($u_l^2 \sim l^{2/3}$, see (9)). The smallest vortices play a fundamental role which is to regulate the energy at the end of its process of injection/transfer/dissipation. But the energetic content of these scales is evanescent and their measurement is a feat that can be judged to be of no value in the case of free flows such as the wake of an object (Figure 1) or in a mixing layer (Figure 3).

But we will see however, that resolving these small scales is of primary importance for wall flows.

Wall flows

On the upstream part of the sphere (Figure 1a), or on the flat plate upstream the rounded ramp (Figure 3a, $X < 0$), the flow is attached and the scales of motion are constrained by the proximity of a solid wall and by the adherence condition $u(z \to 0) = 0$. These flow regions are called boundary layers. This situation is summarized in Figure 5a: when a fluid flows with a velocity U_0 above a solid surface located at $z = 0$, viscous friction, which slows down the flow, is propagated over a thickness δ which defines the boundary layer thickness (usually defined by $u(z = \delta) = 0.99\, U_0$).
In agreement with the preceding, we can seek the smallest scales of the movement taking as a hypothesis that the flow is turbulent, as in Figure 5b.

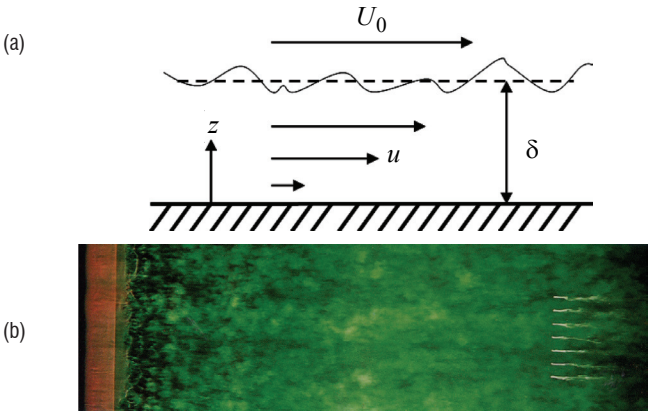

Figure 5 - Boundary layer : (a) definitions, (b) dye visualization of a turbulent boundary layer on a NACA0012 airfoil for a Reynolds number $\mathrm{Re}_c = U_0 c/\nu = 300\,000$, where c is the chord of the profile (view from above; the left and right limits of the image correspond to the leading and trailing edges of the airfoil; taken from Werlé, 1987).

To do this, we must evaluate the length scale l_0 and the velocity scale u_0 which characterize the process of energy injection in the turbulent cascade. For the length scale, one can remark that the physical distance to the wall prevents the motion from developing vertically. The scale of injection of the turbulent energy is thus variable according to the altitude, and we have:

$$l_0 \sim z \tag{14}$$

The evaluation of the corresponding characteristic velocity characterizing the input of energy is a delicate point. Following for example the argument of Landau & Lifchitz (1971), we must remark that the variability of the flow over the thickness of the boundary layer, i.e. between $z = 0$ and δ, is an effect that is caused by the action of the viscous friction on the wall. This introduces the wall friction $\tau_0 = \mu\, \partial u/\partial z\,(z = 0)$ where μ is the dynamic viscosity (the kinematic viscosity being $\nu = \mu/\rho$) as a scaling parameter of the problem. This dynamic parameter allows us to define a characteristic velocity scale: putting $\tau_0 = \rho u_0^2$, we obtain an 'external' velocity scale u_0 of the energy cascade in the form

$$u_0 \sim \sqrt{\tau_0/\rho} \equiv u_\tau \tag{15}$$

This velocity is called the friction velocity and its evaluation usually requires experimental measurements. In that respect, the following reasoning may be considered. If we assume that the flow is turbulent, it must develop an inertial cascade as described previously. The flow at these scales no longer explicitly depends on viscosity ; its properties are only fixed by u_τ and z. For example, the dissipation occurs with a rate $\varepsilon_0(z) \sim u_\tau^3/z$ and the shear $\partial u/\partial z$ must verify $\partial u/\partial z \sim u_\tau/z$. Integrating this latter relation leads to $u(z) \sim \log z$. Therefore, if the flow is turbulent, its velocity must be distributed logarithmically. This is indeed confirmed by the measurements, as will be seen below. Note that these functions do not diverge when $z \to 0$ because there is a minimum physical distance $z_{\min}$ where the flow ceases to be turbulent under a strong action of viscosity. By definition, at this distance the local Reynolds number must be of order unity, i.e. $\mathrm{Re}_{\min} = u_\tau z_{\min}/\nu \approx 1$. Hence:

$$z_{\min} = \nu/u_\tau \tag{16}$$

This scale characterizes the thickness of the laminar sub-layer found at the bottom of boundary layers. To evaluate it, we measure the distribution of velocity u as a function of z and smooth the turbulent fluctuations by taking a time average $< u >$ of u on a sufficiently long period.

We now have enough elements to give some orders of magnitude of the flow scales in a boundary layer, particularly the minimum scale $z_{\min}$ that separates the laminar region from the turbulent one.

Table 1 reports dimensional and non dimensional quantities that characterize three boundary layers of increasing Reynolds number. The first and the third cases are illustrated by the diagrams in figures 6 and 7. These are measurements made with Laser Doppler Velocimetry (LDV) specially adjusted to near wall approaches by minimizing the measurement volume. Following the above dimensional analysis, we traced in these two figures the mean velocity, its standard deviation and the height normalized by their respective reference scales (15) and (16) :

Case	U_0 (ms^{-1})	u_τ (ms^{-1})	$\frac{u_\tau}{U_0}$	$z_{\min}$ (μm)	$z_{z^+=15}$ (μm)	ϕ_v^+	δ (mm)	θ (mm)	Re_θ
1	10	0.46	21.74	33	500	1.2	21.4	25.25	1500
2	40	1.67	23.95	9	135	4.4	16.9	1.57	3400
3	240	9.24	25.97	1.6	24	50	3.46	0.38	6015

Table 1 – Characteristic scales in three boundary layers. Case 1 corresponds to Figure 6, and case 3 to Figure 7. ϕ_v^+ designates the characteristic scale of the LDV measurement volume normalized by the viscous length scale $z_{\min}$. The other parameters are defined in the text. Note the values of the minimal scales $z_{\min}$ (wall unit lengthscale) and $z_{z^+=15}$ (height of the turbulence production region) as well as their reduction when the Reynolds number increases (Losfeld et al. 2003).

$$u^+ = < u > / u_\tau \qquad (17a)$$

$$u'^+ = \sqrt{< u'^2 >} / u_\tau \qquad (17b)$$

$$z^+ = z / z_{\min} = u_\tau z / \nu \qquad (17c)$$

As seen in (17c), z^+ is the Reynolds number that characterizes the flow at height z. Its upper limit, $\delta^+ = \delta / z_{\min} = u_\tau \delta / \nu$, provides a Reynolds number for the whole boundary layer. As the determination of δ and u_τ are generally tricky, it is more convenient to use an integral scale, called momentum thickness, in order to compare various boundary layers:

$$\theta(x) = \int_0^\infty \frac{u}{U_0}\left(1 - \frac{u}{U_0}\right) dz \qquad (18)$$

This provides the values of the Reynolds number $\mathrm{Re}_\theta = U_0 \theta / \nu$ listed in Table 1.

In agreement with the above theoretical prediction, we see in figures 6 and 7 that the measured mean velocity follows a logarithmic law in the region $1 << z^+ << \delta^+$ where a turbulent cascade is possible. In the example of Figure 6, δ^+ is small and the logarithmic region extends over about a decade in z^+. In Figure 7, the Reynolds number $\mathrm{Re}_\theta = U_0 \theta / \nu$ is four times higher (this flow is produced in a transonic wind tunnel ; its Mach number is $M = 0.6$). As the friction velocity u_τ increases with the Reynolds number, the viscous scale $z_{\min}$ decreases, see (16), and the extent of the logarithmic region increases. At $z^+ = O(1)$, by definition, turbulence disappears. A Taylor-expansion then leads to $\tau(z) = \mu \partial u / \partial z(z) \approx \tau_0 z$, whence $u^+ \approx z^+$. This is indeed what is seen in Figure 6a where this linear law is characterized. In the case of Figure 7, the viscous scale $z_{\min}$ falls below 2 μm (!), see Table 1. In this case, the measurement system is no longer capable of characterizing the flow in the laminar sub-layer.

With regard to the fluctuations indicated in the right sides of figures 6a and 7a, we note some remarkable facts. First, the maximum intensity of the fluctuations is not obtained in the fully turbulent region, but at the level of its lower boundary, i..e. at about $z^+ = 15$. This corresponds to about $z = 500$ μm in case No. 1 and $z = 24$ μm (!) in case No. 3. This is the most unstable region of the flow, where production of the fluctuation energy of the turbulent boundary layer is maximal. Lastly, figures 6b and 7b show the probability density functions of the velocities measured at various heights. These distributions become singular in the laminar regions $z^+ = O(1)$ and $z^+ = O(\delta^+)$, and their enlargement in the regions where turbulence may develop characterizes the richness in scales of the turbulent process. Note that most of these histograms are skewed and deviate from a Gaussian distribution: this is one of the characteristics of turbulent shear flows.

The limits of flow simulation

We will now show that to capture all turbulent scales in a turbulent flow, from the larger to the smaller, supercomputers are indeed necessary. In accordance with (12), the minimum number N_{pt} of nodes required to capture all details of a turbulent flow is:

$$N_{pt} \sim \left(\frac{l_0}{\eta}\right)^3 \sim \mathrm{Re}_0^{9/4} \qquad (19)$$

For the case of Figure 1 where $\mathrm{Re}_\theta = 400\,000$, this gives $N_{pt} \approx 4\,10^{12}$ nodes. Furthermore, to solve the Navier-Stokes equations (1) with a numerical method, a minimum number of time steps is also necessary. It can be demonstrated that this number verifies $N_t \sim \mathrm{Re}_0^{1/2}$. A simulation thus requires a spatio-temporal meshing with at least $N_{pt} \times N_t \sim \mathrm{Re}_0^{11/4}$ points which leads to the astronomical number of 2.510^{15} points to handle the case of a simple sport ball. We are still far from having the technology needed to do this. Not to speak of an aircraft, for which Re_θ can reach 10^9, or even a car, for which $\mathrm{Re}_0 \approx 10^7 - 10^8$. Now think of the atmosphere…

Figure 6a gave an example of a direct numerical simulation of a boundary layer sufficiently resolved in 1990 thanks to its moderate Reynolds numbers. Note that once validated, such a direct simulation (DNS), free of any modeling, became a reference because it provides information on quantities that are not measurable. Case of Figure 7 has a larger Reynolds number and requires a meshing that is about 20 times denser. Such a case can be simulated nowadays. But we should now remember that this is just a boundary layer on a smooth flat plate.

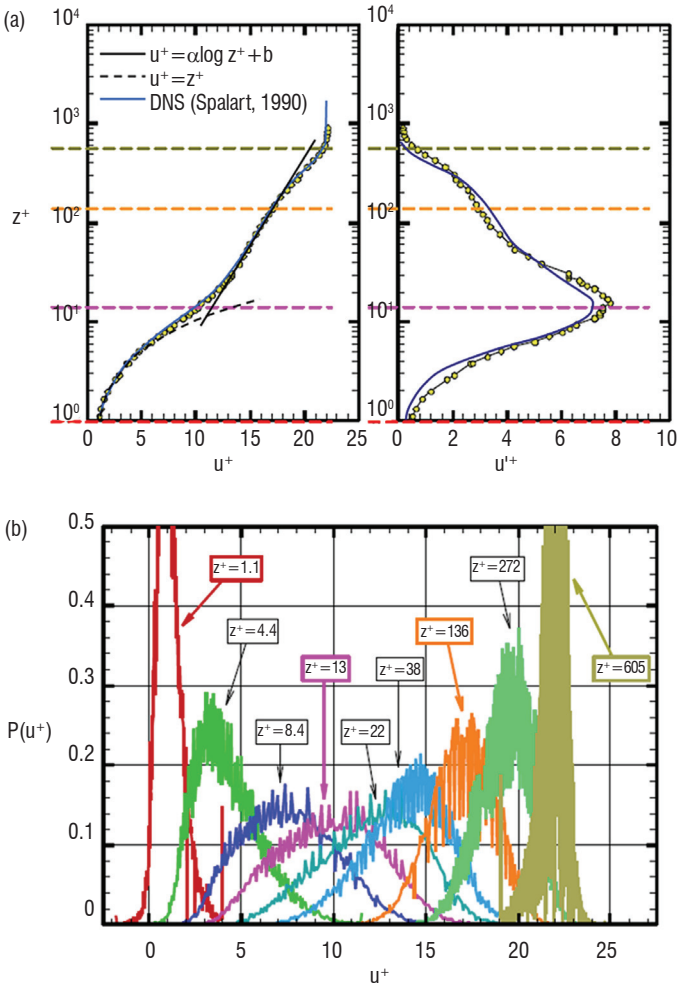

Figure 6 – LDV measurements in an incompressible boundary layer (case N°1 of table 1 : $U_0 = 10$ ms^{-1}, $\mathrm{Re}_\theta = 1500$): (a) average (left) and standard deviation of the fluctuations (right) of the longitudinal velocity component in wall variables and comparison with a direct simulation done at $\mathrm{Re}_\theta = 1410$ (Spalart, 1990), (b) probability density function of the fluctuations at various altitudes. The characteristic scale of the measurement volume is $\phi_v = 40$ μm, to be compared with the viscous scale $z_{\min} = 33$ μm ($\phi_v^+ = 1.2$, see Table 1). Taken from Losfeld et al., (2003).

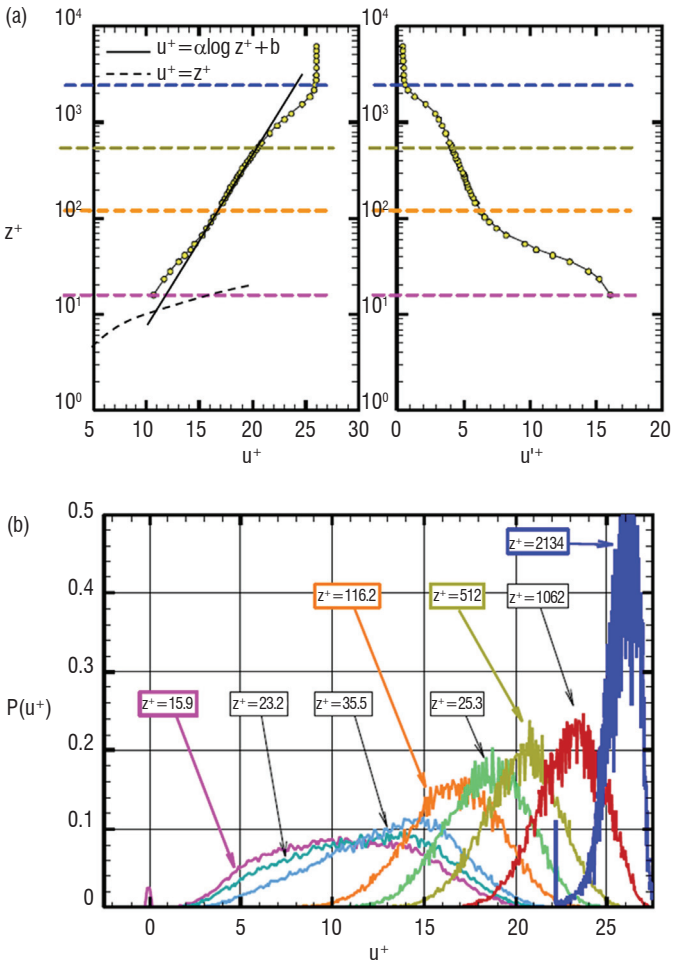

Figure 7 – LDV measurements in a compressible boundary layer (case N°3 of table 1: U_0=240 ms^{-1}, Re_θ=6015): (a) average (left) and standard deviation of the fluctuations (right) of the longitudinal velocity component in surface variables, (b) probability density function of the fluctuations at various altitudes. The characteristic scale of the volume of measurement is ϕ_v =80 μm, to be compared to the viscous scale $z_{\min}$ =1.6 μm (ϕ_v^+ =50, see Table 1). Taken from Losfeld et al. (2003).

These limitations not only concern computing time, but also data storage. For each time step and at each point where we solve the equations of fluid mechanics, we must store the three components of velocity and pressure. If the flow is not incompressible, we must add temperature and density. This means recording four or six variables, to which we must add the four indices of the node (space and time), which becomes soon an unmanageable problem. Besides, we are just speaking here of a non-electrically charged and non-reacting flow. This gives an idea of the extent of the problem of simulating (and measuring) high Reynolds number flows from a practical standpoint.

In light of these difficulties, over the course of history, the Navier-Stokes equations were degraded by means of various statistical filtering methods. The success of these methods seems to be guaranteed by the apparently stable and repeatable nature of the statistical properties of turbulent flows (turbulent motion, which is chaotic if we try to follow a trajectory, becomes stable in the sense of ensemble statistics ; we thus realize, at the risk of destroying a stereotype, that turbulence is a fundamentally regularizing process). The activity which consists in formalizing the 'turbulent' terms of the equations resulting from these filtering operations is referred to as 'turbulence modeling'; A great research effort has been made on turbulence modeling in the 1980-90's. It led in particular to the current steady calculation methods, called RANS methods (for Reynolds Averaged Navier-Stokes). The calculation of the flow around a complete aircraft is now feasible thanks to such methods. But models become ineffective when turbulence is not in equilibrium, as it is often the case when it is subjected to mechanisms such as rotation, curvature, compressibility, shock waves, heat release, etc, or when it is no longer separable without ambiguity from a mean field, as is the case in highly unsteady flows. In such cases, turbulence can no longer be easily integrated into an artificial viscosity or in an inter-scale transfer function that are the artifacts used in most practical simulation tools. The success of the simulation then depends on the 'know-how' of the operator who must choose the best compromise among the tools at his disposal. But this also depends on the operator's physical knowledge of the simulated problem and on the availability of measurements he can validate his choices with.

Metrology is challenging flow physics

In the context of the massive investment of computational fluid mechanics which characterizes now the discipline, the role assigned to experimentation has evolved. In recent years, its role has been mainly to validate the numerical solutions by providing information needed for calibration of specific physical models. For instance, flow surveying by LDV played a major role in the development of RANS methods by allowing to measure with a high accuracy the statistical moments of velocity involved in the RANS equations. But measurements are also constantly challenging the researcher and accompanying him in both his theoretical analyses and modeling efforts. This is exemplified by PIV, a technique which is supplanting progressively LDV: while the commercial success of PIV came from a significant reduction of operational difficulties (compared to LDV), it opens up new possibilities that are not covered by the current simulation tools and their modeling capacities. In a near future, thanks to continuous progress in the field of lasers and digital cameras, PIV should provide a direct and complete description of the spatio-temporal kinematics of turbulent flows. Only direct numerical simulation of the Navier-Stokes equations (DNS), which is model-free, could be comparable to this. The current limitation of PIV lies in the handling of the considerable mass of data it produces. What can we do with all this information? What kind of model could use it? We should expect that PIV will contribute to modifying the landscape of modeling in fluid mechanics by giving rise to new theoretical proposals. Presently, on the fundamental basic research side, PIV is already at the core of modern analyses of hydrodynamic stability and flow control.

Conclusion

In this article, we first presented the physical principles that determine the characteristic scales of monophasic and incompressible flows at high Reynolds numbers, which are that found in wind tunnel experiments. The key analysis tool is the famous phenomenological theory of Kolmogorov, the basics of which we have outlined. The two experiments used here to illustrate the introduced concepts involve three main velocimetry techniques of fluid mechanics: PIV, LDV and hot wire anemometry. Note that beyond the limited framework of monophasic flows considered here, specific measurement methods exist to investigate multiphase flows, reactive flows, or plasmas; other physical scales are involved in these problems, which make the measurements more complex. Finally, we emphasized how challenging turbulence is for computational fluid mechanics and how important measurement is for the stimulation and development of scientific research in fluid mechanics ■

Acknowledgements
The author would like to thank his PhD student Benoit Gardarin and his colleagues Gilles Losfeld and Philippe Geffroy for kindly providing him with the two data commented on in this article. Benjamin Leclaire is acknowledged for his useful remarks.

References
[1] B. GARDARIN, L. JACQUIN - *Flow Separation Control with Vortex Generators.* AIAA-4th Flow control conference, Seattle, 23-26 June 2008.
[2] L. JACQUIN, P. TABERLING - *Turbulences et tourbillons.* Cours de l'école Polytechnique, édition 2006.
[3] G. LOSFELD, F. MICHELI, P. GEFFROY, R. SOARES, Y. LE SANT - *Vélocimétrie laser à frange, amélioration des mesures en couche limite.* Rapport Technique Onera N° RT 223/07382, DAFE, December 2003.
[4] A.N. KOLMOGOROV - *The Local Structure of Turbulence in an Incompressible Fluid with Very Large Reynolds Numbers*. Dokl. Akad. Nauk. SSSR, vol. 30, pp. 301-305, 1941.
[5] LANDAU, LIFCHITZ - *Physique théorique*. vol.6: Mécanique des fluides, Editions Mir, 1971.
[6] L.F. RICHARDSON - *Weather Prediction by Numerical Process*. Cambridge University Press, 1922.
[7] P. SPALART - *Direct Simulation of Turbulent Boundary Layer up*. Journal of Fluid Mechanics, 187, 1988.
[8] H. WERLÉ - *Transition et turbulence*. Note Technique 1987-7, Onera, 1987.

Acronyms
PIV (Particle Image Velocimetry)
RANS (Reynolds Averaged Navier-Stokes)
LDV (Laser Doppler Velocimetry)
DNS (Direct Numerical Simulation)

AUTHOR

Laurent Jacquin Research Director, Director of the Fundamental/Experimental Aerodynamics Dept of Onera. Associated Professor in Mechanical Engineering at Ecole Polytechnique (from1996 to 2007). Background: Master Degree in Mechanical Engineering from University of Marseille. PhD from University of Marseille in 1983. Research Habilitation Thesis (thèse d'état) from University of Lyon in 1987. Joined Onera in 1987.
Research topics include: Turbulence, Hydrodynamic stability, Vortex Dynamics, Compressible Flows, Aerodynamics, Experimental Methods.